

Improving SNR in a HF Link with Circularly Polarized Antennas

A Major Qualifying Project submitted to the faculty of Worcester Polytechnic Institute in partial fulfillment of the requirements for the Degree of Bachelor of Science in Electrical Engineering

Drew Schoen O'Shaughnessy
October 2019

This report represents the work of WPI undergraduate students submitted to the faculty as evidence of completion of a degree requirement. WPI routinely publishes these reports on its website without editorial or peer review. For more information about the projects program at WPI, please see

<http://www.wpi.edu/academics/ugradstudies/project-learning.html>

Abstract

There are several challenges associated with establishing reliable radio communication in the High Frequency (HF) bands over an ionospheric channel. Fading due to phase cancellation of left-hand and right-hand circularly polarized waves at the is one such problem. In an effort to reduce fading, several over-the-air transmission tests were performed with orthogonal receive antennas. Signal processing was performed on the recorded IQ data using MATLAB scripts so that the improvement in the signal-to-noise ratio could be quantified. Additionally, several off-the-shelf linear antennas were characterized using EZNEC and Altair FEKO for circular polarization performance when used in a crossed configuration.

Acknowledgements

I would like to thank...

- Ian Gelman for his help in answering questions about signal processing and suggesting faster filtering functions in MATLAB.
- Eliot Lebsack of the MITRE Corporation for overseeing this project, answering my many questions, and help in the execution of this experiment.
- MITRE department T823 (Sensors, Electromagnetics, and EW) for sponsoring this project.
- Professor Alexander Wyglinski for answering questions about the content and structure of this report.
- Cecelia Franzini of the MITRE Corporation for reviewing this paper and offering many helpful suggestions.

Contents

1	Introduction	1
2	Theoretical Background	2
2.1	The Ionosphere	2
2.1.1	D Layer	3
2.1.2	E Layer	3
2.1.3	F Layer	4
2.1.4	Solar Weather and the Ionosphere	4
2.2	Polarization Fading	4
2.3	Circularly Polarized Antennas	5
2.4	Findings From Other Studies	5
3	Experimental Process	6
3.1	Test Objectives	6
3.2	Test Locations	6
3.2.1	Transmitters	6
3.2.2	Transmitters of Opportunity	6
3.2.3	Receiver Location	7
3.3	Test Equipment	7
3.3.1	Transmitting Equipment	7
3.3.2	Receiving Equipment	7
3.4	Test Procedure	7
3.4.1	Characterization of the Ionosphere Using Ionosondes	8
3.4.2	Reception Using WBHF SDR	8
3.4.3	Reception Using 0-90 Hybrid Coupler	9
3.5	Processing for SNR Metrics	9
3.5.1	General Processing Method	9
3.5.2	Processing in the Presence of Interference	11
3.5.3	Reconstruction of Circularly Polarized Waves	12
4	Results	13
4.1	Preliminary Findings	13
4.1.1	WWV	13
4.2	Theoretical Improvements from Antenna Simulations	13
4.2.1	EZNEC Model	14
4.2.2	Altair Feko Model	16
4.3	Test Results	17
4.3.1	Reception with Software Reconstruction of Circular Polarization	17
4.3.2	Reception with 0-90 Hybrid	20
5	Conclusions and Recommendations	21
	Appendices	23

A White Wolf Systems “Whiskey” Antenna	23
B MATLAB Scripts	24

List of Figures

1	Relative Heights of the Layers of the Ionosphere [5]	3
2	Visualization of O and X Mode Polarization	4
3	Program Flow for <code>snr_vs_time_batch.dat.m</code>	11
4	Example of Vector Rotation	12
5	Two WWV Samples	13
6	EZNEC Model of the MITRE Crossed Dipole	15
7	MITRE Crossed Dipole Elevation Far Field, 5 MHz	15
8	MITRE Crossed Dipole Elevation Far Field, 7 MHz	15
9	Feko Model of the MITRE Crossed Dipole	16
10	MITRE Crossed Dipole Elevation Far Field, 5 & 7 MHz	16
11	Data From Test on September 12, 2019	18
12	Ionograms During September 12 Tests	18
13	Data From Test on September 20, 2019	19
14	Ionograms During September 20 Tests	19
15	Ionograms During Tests with 0-90 Hybrid	20
16	EZNEC Model of the Whiskey Antenna	23
17	Whiskey Elevation Far Field, 5 MHz	23
18	Whiskey Elevation Far Field, 7 MHz	24
19	Feko Model of the Whiskey Antenna	24
20	Whiskey Elevation Far Field, 5 & 7 MHz	24

Acronyms

AM Amplitude Modulation. 13

EZNEC Easy Numerical Electromagnetics Code. 14, 16

FFT Fast Fourier Transform. 10

HF High Frequency. 1

LHCP Left Hand Circular Polarization. 5, 9

MoM Method of Moments. 14, 16

MUF Maximum Usable Frequency. 9

NEC Numerical Electromagnetics Code. 13, 14

NVIS Near Vertical Incidence Skywave. 5, 14

RHCP Right Hand Circular Polarization. 5, 9

SNR Signal to Noise Ratio. 5, 6, 9–11

WBHF Wide Band HF. 9, 10, 12, 13, 20

1 Introduction

The High Frequency (HF) band spans formally from 3 MHz to 30 MHz. It is used extensively by military, government, and amateur users for long distance communication with no intermediate infrastructure. The band is unique among all radio spectrum because of this potential for long distance communication. The natural phenomena by which this long distance communication happens is ionospheric refraction of the electromagnetic waves.

Although radio communication over HF might bring to mind images of antiquated or out-of-date technology, HF is still an extremely popular communications band when wireless long distance communications are needed. One such example is the High Frequency Global Communications System, operated by the United States Air Force. This communications system uses several frequencies in the HF band to relay messages, provide phone patch service, and offer several forms of data connectivity to and from airborne aircraft and ground stations. [1] These transmissions, especially the Emergency Action Messages, are well known by shortwave listeners and amateur radio operators alike.

Amateur radio operators could be considered the first users of this frequency spectrum. In the earliest days of radio, frequencies above several hundred kilohertz (in the Medium Frequency and Low Frequency bands) were difficult to use, in part because oscillator technology was not mature enough, and the propagation of radio waves was not well understood. It was thought that shorter wavelengths did not travel as far, and thus were not investigated for commercial interests. Amateur radio stations were eventually relegated to wavelengths below 200 meters by the Radio Act of 1912.

The famous radio pioneer Guglielmo Marconi made the first successful transatlantic radio broadcast in 1901. At that time, radio waves were not thought to travel beyond the horizon, or the line-of-sight. This discovery led to the proposal of an atmospheric layer which reflected radio waves which facilitated Marconi's experiment. This layer came to be known as the Kennelly-Heaviside layer, after the two scientists who proposed its existence.

Since this time, the propagation of radio waves has become very well understood both by scientists and amateurs. The Kennelly-Heaviside Layer is now known to be the F layer, which is one of four layers that compose the ionosphere. Continuous use of this layer in later decades proved to be a fairly reliable method of long distance communication for the time. However, current understanding says that the ionosphere does not facilitate radio wave propagation at all times of day, at all points on the Earth, on all frequencies. Signals will often experience fading as they travel from one point to another via the ionosphere. This has been mitigated to an extent by using different frequencies during different times of the day to counteract the frequency dependence of the different layers of the ionosphere. However, there are other possible causes of fading, such as the destructive interference of oppositely polarized waves.

In this report, destructive interference (fading) due to the cancellation of right-hand and left-hand circularly polarized waves will be discussed. An attempt is made at mitigating this fading using a crossed dipole as a receive antenna in a HF radio link.

2 Theoretical Background

This chapter will introduce some parts of electromagnetic theory and wave propagation theory which are necessary to understanding this project. First, the general nature of the ionosphere will be explained, before taking a closer look at the more complex properties that it has. Each ionospheric layer will be described briefly.

This project centers heavily around the issue of signal fading as a result of ionospheric influence. Fading can be caused by a number of different mechanisms. However, in this project, the primary research objective is minimizing fading caused by the destructive interference of circularly polarized waves. This fading phenomena will be discussed in the second subsection.

In the third subsection, some discussion on the general geometry of circularly polarized antennas will be made to motivate their usage and understand their design. Finally, conclusions from a similar study will be discussed.

2.1 The Ionosphere

The ionosphere is defined in [2] as “that part of a planetary atmosphere where ions and free electrons are present in quantities sufficient to affect the propagation of radio waves.” In what part of the atmosphere of Earth does the ionosphere really exist? To understand the formation and properties of the ionosphere, we must first examine the composition of the atmosphere.

Earth’s atmosphere is composed primarily of the following four species. [3]

Species	%
Molecular Nitrogen	78.08
Oxygen	20.95
Argon	0.93
Carbon Dioxide	0.04

These percentages are valid for the atmosphere that exists below the mesopause. Above the mesopause, molecular O₂ is broken by the constant bombardment of ionizing UV radiation coming from the Sun. At these altitudes and pressures, atoms do not recombine as readily and thus atomic oxygen becomes a much larger percentage of the total composition. [4] The constant ionization happening here introduces free electrons into the atmosphere, creating a charge density wherever the ionization is occurring.

The density of all gases lessens with increasing altitude as a result of the lessening gravitational pull from the Earth. The atmospheric pressure also decreases with altitude, but not monotonically. The density of free electrons will also vary in accordance with the local gas density and pressure.

The combined effects of ionizing radiation and varying density and pressure give rise to a layered structure within the ionosphere. In turn, the effect that each layer has on an incident electromagnetic wave varies greatly as a function of frequency, electron/ion density, and height.

The ionosphere has three distinct layers, first labelled by Edward Appleton as E and F, for ‘electric’ and ‘field.’ Upon the discovery of a lower absorptive region, he chose D to keep

with the convention. These layers exist as D, E, and F in order of increasing height above the surface of the earth. Incoming solar radiation (primarily cosmic rays, X rays, and ultraviolet light) helps to ionize oxygen atoms and other molecules. Ionization happens more readily as a result of the lower density of gases at these heights. The great number of free electrons in the ionosphere create the conditions necessary for the enhancement and the refraction of radio waves.

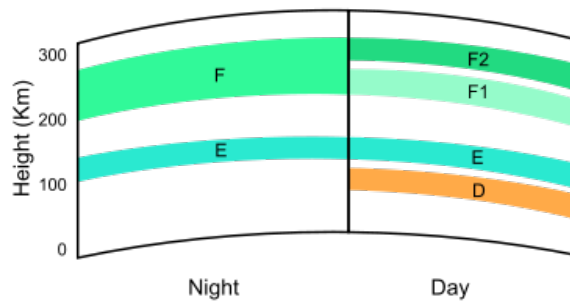


Figure 1: Relative Heights of the Layers of the Ionosphere [5]

2.1.1 D Layer

The lowest region is the D layer. This layer sits at approximately 50 km to 90 km in height. The D layer is responsible for the absorption of frequencies above LF. The D layer is present only during the daytime, when ionizing radiation from the sun impacts the molecules and frees electrons. These free electrons receive energy from incident radio waves, which move them so that they recombine with the nearby molecules in the denser atmosphere, dissipating the energy from the wave. During the night, when electron recombination in the D layer is much lower, the D layer will not absorb but reflect frequencies in the lower portion of the HF band. Higher frequencies are still attenuated. [4]

2.1.2 E Layer

The next highest region is the E layer. The E layer exists approximately between 90 km and 140 km above the surface of the Earth. The E layer exists due to soft X-rays from the sun ionizing oxygen molecules between these altitudes. The E layer exhibits almost opposite propagation characteristics as the D region. Frequencies below 10 MHz are reflected off this layer, and higher frequencies are absorbed. The E layer still exists during the night, even though it does not receive X rays from the sun. However, during this time the average height of the E layer rises, which has the effect of compensating for the diminished ionization activity by allowing signals to propagate farther. A higher reflecting layer allows for a longer theoretical single hop bounce. [4]

Sporadic E is a special case of E layer propagation which allows for the refraction of electromagnetic waves that are well into the VHF band. Sporadic E has earned its name for the very short duration and highly variable locations at which this propagation mode

occurs. Sporadic E propagation happens exclusively during the daytime. This propagation is caused by a sudden local increase of the electron density in the E region. [4]

2.1.3 F Layer

The highest layer in the ionosphere is the F layer. The F layer exists above approximately 140 km, and the ionization of oxygen atoms here is caused primarily by extreme ultraviolet radiation. The F layer is present during both the day and the night, but during the day, this layer splits into two sub-layers, labelled F_1 and F_2 . This layer is responsible for the majority of long-distance HF communication, because it supports refraction of frequencies up to the top of the HF band. Because it is the highest layer, it also supports the longest single hop propagation, which is estimated to be a maximum of 4000 km.

2.1.4 Solar Weather and the Ionosphere

The ionosphere is also greatly influenced by solar weather. Coronal mass ejections and solar wind fluctuations have tremendous effect on the electron density and overall charge distribution of the ionosphere. In extreme solar weather, such as a solar flare, the incoming radiation penetrates down to the lower D and E layers and causes additional ionization there. Normal communications that would take place via the F layer are now inhibited. Such an event is known as a radio blackout. [6]

2.2 Polarization Fading

In the preceding sections, it has been established that wave propagation through the ionosphere has many variables, all of which will affect the strength of the signal at the receiver. Many of these fading mechanisms can be considered absorptive fading mechanisms. However, there are several other non-absorptive fading mechanisms. Fading can occur due to interference of other waves reflecting off of an irregular ionospheric boundary. Additionally, signals can undergo fading as a result of polarization fading, which occurs as a result of phase differences between O and X mode waves.

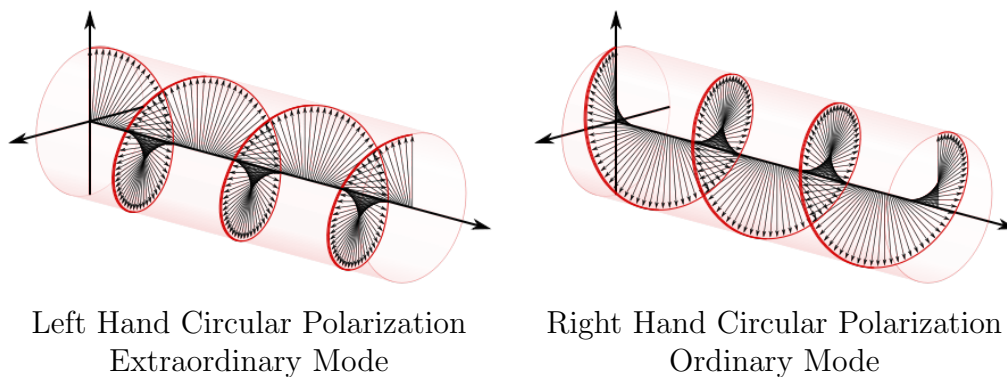


Figure 2: Visualization of O and X Mode Polarization [7], [8]

]

A linearly polarized wave can be considered as the sum of both a right hand and a left hand component that rotate in opposite directions. The vector sum of these oppositely rotating right- and left-hand field vectors oscillates along a line (one dimension) as the wave propagates through space. When there exists a phase difference between the components, the E and H field vectors interfere destructively with one another and no longer oscillate in one dimension. Significant attenuation can occur when the rotating field vectors are properly phased. [4]

Amplitude imbalances between the left and right hand components also cause the resultant wave to be elliptically polarized. This is also a probable cause of fading, since the amplitude of an incoming wave is also subject to the aforementioned absorptive effects. The more elliptical an incoming wave is, the more energy is taken from the linear component of the wave that aligns with the linear receiving antenna.

2.3 Circularly Polarized Antennas

Antennas designed for circular polarization can aid in rejecting one of the circular components. Such antennas are designed to respond to one polarization only by cancelling the other component, commonly through a 90 degree phasing technique. In the simplest case, two orthogonal dipoles can be utilized with a phase shift to cancel one component. In design examples where a wide bandwidth is not needed, a quarter wave transmission line can be used to obtain the 90 degree shift. Other phasing methods such as a 0-90 hybrid can be used as well. More complex antenna geometries (such as the helix and the spiral) can be used to generate circular polarization. However, they are impractically large at the wavelengths required for HF, and thus rarely used in this frequency range in comparison to linear wire antennas.

2.4 Findings From Other Studies

The subject of this experiment has also been investigated by several researchers from the Netherlands. Their research, while not identical in focus to this experiment, yielded some important conclusions about the use of circular polarization on HF and the isolation that exists between LHCP and RHCP. In their experiment, two HF receivers were used to measure the received signal strength of a beacon transmitter. The receiver and transmitter were separated by a distance of approximately 100 km to ensure NVIS propagation. The beacon transmitter used a simple horizontal half wave dipole at 5.39 MHz. Each receiver used a turnstile antenna, with one configured for left hand and the other configured for right hand circular polarization. The results of this test showed that there was 13 dB of isolation between the modes and an overall SNR improvement of 3 dB when RHCP was used. In addition, the authors stated that fading was less pronounced on the receiver that used RHCP. [9]

3 Experimental Process

3.1 Test Objectives

Fading due to absorptive and refractive properties of the ionosphere is a problem with no complete or immediate solution. Because a user of the HF spectrum is unfortunately at the mercy of the ionosphere, there is little that can be done to eliminate fading and other interference that arises naturally from the properties of the ionosphere. However negative this assessment is, we should not consider the HF spectrum completely unusable.

The objective of this experiment is to investigate how the SNR of an HF radio link can be improved by mitigating fading. As described before, most of the causes of fading are not controllable. However, using circularly polarized antennas on a HF receiver should yield an improvement in the SNR for the channel. This experiment will provide quantitative data to that effect.

3.2 Test Locations

3.2.1 Transmitters

It is not practical to test a HF communications system over a very short range, because the effects of the ionosphere will not affect the radio wave as it travels from the transmitting site to the receiving site. For this experiment, the test transmitter will be located at the Air Force Research Laboratory site in Stockbridge, NY. Locating the transmitter here will ensure that the electromagnetic wave will arrive via the ionosphere and not ground wave propagation.

It is important to note that this experiment will provide more insight to those who wish to gauge performance for shorter ionospheric paths. Such paths are sometimes termed “Near Vertical Incidence Skywave” (NVIS) paths, due to the very small angle of incidence they make with the ionosphere. Stockbridge is roughly 225 miles from Bedford, and thus it is not likely that the radio waves have a low angle of incidence along this path.

3.2.2 Transmitters of Opportunity

Several transmitters of opportunity will be utilized to provide additional data about ionospheric propagation. In addition to the intentional transmissions, the time station WWV will be recorded on 10 and 15 MHz. WWV is one of two standard time stations operated by the National Institute for Standards and Time (NIST). WWV broadcasts continuously from Fort Collins, Colorado, on 2.5, 5, 10, 15, 20, and 25 MHz. This station will essentially serve as a beacon, so that a rough estimation for signal strength and propagation quality can be made. WWV is an excellent station to use as a reference, because it is on a known and stable frequency, broadcasts continuously, and has a known modulation format (AM).

High Frequency Global Communications System (HFGCS) stations will also be recorded. These recordings will not provide as much insight into current propagation quality as the WWV recordings will. This is partly a consequence of the fact that the locations of the transmitters are not identifiable from the signals themselves. The HFGCS network includes airborne aircraft, and numerous Air Force bases across the United States, and thus tracing

a signal back to its origin is not feasible. Although the signals are Upper Sideband (USB) analog voice, the messages are coded and contain no information identifying the origin or destination of the traffic. Thus, these signals can only be used to help in the testing and adjustment of the filters and detection algorithm in the MATLAB scripts.

3.2.3 Receiver Location

The receiver used in this project will be located at MITRE's campus in Bedford, MA.

3.3 Test Equipment

3.3.1 Transmitting Equipment

The transmitter in this experiment is a Harris RF-7800H radio with a 125 watt power amplifier. This is connected to a White Wolf Systems "Whiskey" antenna, which is a broad-band HF antenna with a radiation pattern optimized for high takeoff angles, to enhance Near Vertical Incidence Skywave (NVIS) propagation.

3.3.2 Receiving Equipment

The HF communications link is first established using one of the aforementioned Harris radios. Both are equipped with Automatic Link Establishment (ALE) capabilities which allow the radios to communicate rapidly on a number of predefined frequencies in order to find and select one with no interference, ensuring a high SNR. Once the link is established, the command is manually given to these radios to begin a transmission using the MIL-STD-188-110B waveform.

ALE is not necessary to use in all cases to establish a link. The control software used for these radios in this experiment also allows for the operator to specify a frequency for transmission.

The reception and recording of the IQ data is accomplished using the MITRE Wide Band HF SDR system. This is a dual channel radio system which has two independent hardware receivers. When recording, it allows for two separate IQ data streams to be recorded. Because of the independent receiver hardware, two separate antennas can be used.

For the purposes of this experiment, each channel of the radio has been connected to one half of a MITRE-designed, wide band crossed dipole. This allows for the software reconstruction left hand and right hand circular polarization, and eliminates the need for separate right hand and left hand polarized antennas or 90 degree hybrid combiners.

The MITRE WBHF Testbed has been configured to record spectrum over a bandwidth of 200 kHz, so that an accurate measure of the adjacent noise floor can be made. The samples are then processed on a personal computer in MATLAB, using various functions from the Signal Processing Toolbox.

3.4 Test Procedure

This test will be executed repeatedly over the course of several days, in solar weather conditions that will be largely unpredictable from day to day. It is anticipated that variables

such as the time of day or the terrestrial weather could have some effect on these tests. However, these are not the variables of interest, nor are they expected to have a large effect on the outcomes of the tests. The testing cannot be guaranteed to happen at the same time each day, which means that there will be a different MUF and layer heights for each set of samples. To account for this, ionograms will be recorded with each sample set and included for later reference.

3.4.1 Characterization of the Ionosphere Using Ionosondes

This project has been granted permission to use resources from the MITRE Corporation, including the ability to execute an ionospheric sounding and generate ionograms. An ionospheric sounding involves using a transmitter that generates a chirp, which is a carrier tone that is frequency swept over a defined range. A receiver tracks the carrier and the time difference between transmission and reception is recorded. Ideally, the transmitter and receiver are located such that the electromagnetic wave will arrive via ionospheric propagation and not via ground wave propagation.

Simple ionograms assume a constant propagation speed. Using geometry, the height of a ionospheric layer can be inferred from the recorded time difference. More complex models will factor in slightly varying propagation speeds, as well as multipath or multihop wave paths through the ionosphere. Several faint reflections could be indication of the wave refraction off of the bottom of one layer, the off the top of a lower layer, before going up once more and then down to the receiver.

Using this ionogram data, the ionosphere can be characterized for relevant information such as the Maximum Usable Frequency (MUF) and ionospheric layer height. This data will help to predict the performance of a communication link on a given frequency. The data from the the test link can be correlated with these ionograms.

An ionogram will be observed before each set of test transmissions in order to inform the choice of frequency for the transmissions. Although the Harris radios can utilize ALE to select a frequency automatically, this functionality will not be used. The ALE may select a frequency that supports a channel with extremely good SNR at the instant that the ALE was initiated. But, this frequency could also fall well above the MUF prediction in the ionogram. Thus, the experimenter will set the frequency manually based upon the latest ionogram data. It is recommended that the frequency be chosen in the middle of whatever sounding returns exist on the ionogram. This decision is not made according to a rigorous method, but rather left to the judgement of the operator.

3.4.2 Reception Using WBHF SDR

The second stage of this experiment will be collecting recordings of a data waveform, transmitted from the test transmitter over the predefined test frequencies, and recorded in Bedford, MA.

The sending and receiving of the data waveforms for this experiment is done manually by the operator. The transmitting radios are first initiated by the operator, and then manually invoked to send a data packet. The duration of a test transmission normally takes less than 20 seconds. The receiver is also manually invoked before the command to transmit is given,

and then terminated after the transmission is done. In this step, the receiving SDR will be recording the transmission between the two Harris radios, using the crossed dipole as described.

3.4.3 Reception Using 0-90 Hybrid Coupler

In the final stage of the experiment, the Harris radio will be connected to the crossed dipole via a 0-90 hybrid coupler, to take full advantage of the rejection of one circular polarization. This extra test may seem redundant given that both left hand and right hand circular polarization can be reconstructed digitally using the WBHF Testbed. However, it is desirable to run an experiment using something that more closely resembles an actual usage scenario, even if it will not provide any new data. Thus, the Harris radio will be used instead of the WBHF Testbed and there will be separate test transmissions using both linear polarization and circular polarization, enabled by the hardware 0-90 hybrid device.

The test will be completed as follows. First, an ionospheric sounding will be executed to determine a frequency on which the test transmissions will take place. Once a frequency has been chosen, two test transmissions will occur, each with different phasing of the antenna arms. This will determine which configuration is RHCP, or X mode propagation. The X mode propagation should be the mode with higher SNR.

Another sounding is then executed. Soundings will occur between each iteration of the test to ensure that an optimal frequency is chosen. One transmission involves switching cables on the the 0-90 hybrid and communicating with the operator who is giving the command to send the messages. During this time, ionospheric conditions could change enough to make the previously chosen frequency too close to the MUF. A new frequency will be chosen if it is decided that the previous one is no longer optimal.

Now that frequencies have been decided upon, the test transmissions will begin and the SNR will be recorded for each. The first transmission will take place using RHCP (X mode). The second transmission will take place using linear polarization, so that a baseline can be established. It is important to have this baseline because part of the goals of this experiment is to quantitatively measure the performance of circular polarization over linear polarization, not just one circular polarization over another. The linear antenna will be the arm of the MITRE Crossed Dipole that is oriented broadside to the direction of the incoming wave.

Two RHCP (X mode) and one LHCP (O mode) transmissions will take place to confirm the first X mode SNR data, as well as collect data to establish the performance difference between the X and O propagation modes.

Once the resulting signal data has been recorded, the SNR data from the tests with the WBHF Testbed will be compared with that of the tests using the 0-90 hybrid. This test will be repeated as necessary to obtain clear and decisive data.

3.5 Processing for SNR Metrics

3.5.1 General Processing Method

The resultant signals are processed in MATLAB using functions from the Signal Processing Toolbox. The object of this processing is to ascertain which polarization provided

the best Signal to Noise Ratio (SNR). SNR has a fairly simple definition: the ratio of signal power to noise power within a given bandwidth. Because of the high dynamic range of RF signals, this ratio is most often expressed in decibels.

This definition puts some requirements on the way that these samples are to be processed. The first requirement is to acquire a sample of noise that corresponds with the amplitude of the actual noise floor, but in a bandwidth equivalent to that of the signal. The bandwidth of the MIL-STD-110B waveform is approximately 4 kHz; therefore, a noise sample over a bandwidth of 4 kHz is also needed. The simplest solution was to use a bandpass filter to sample the noise floor over an adjacent span of 4 kHz, and use this as the noise sample. The bandpass filter was positioned far enough away from the signal of interest so that the signal would not appear very close to the passband region.

The MATLAB scripts written for this processing were written to run automatically and process a large batch of samples. This batch processing methodology does fail to produce accurate results when there happens to be another signal or anomalous interference in the passband of the filter responsible for producing a noise sample. This will be discussed further in Section 3.5.2.

The WBHF Testbed is configured to mix the received signal down to 0 Hz. It is effectively a single conversion receiver. For this reason, a simple low pass filter can be used to obtain the desired signal.

The functions used to create the filters are from MATLAB's Signal Processing Toolbox. The filter coefficients for both filters are generated using `designfilt`. The requirements for the filters themselves need not be incredibly strict; any filter that can attenuate adjacent signals by 60 dB or more will suffice. For this reason, Butterworth filter coefficients are used. Several standard filtering functions were tried initially, including `lowpass` and `bandpass`. However, these filter functions are much more computationally intensive than other filtering functions and do not allow for finer control of the filter specification. [10] For this reason, filtering is completed by `fftfilt`, which uses a Fast Fourier Transform (FFT) based multiplication method to filter signals in a very computationally efficient method, when compared to time domain based filtering methods. [10] Once the filtering is complete, the filtered samples are compared in MATLAB's `snr` function. This function computes "... the ratio of the summed squared magnitude of the signal to that of the noise." [11]

It is important to note how the SNR is calculated. The SNR is not calculated blindly across the entire duration of the sample. This would yield a very inaccurate number, because the signal is not present for the entire duration of the sample. Within the script used to process the recorded signals, a simple detection scheme is implemented to track the beginning and end of the signal:

1. Compute SNR for the entire sample.
2. Take average SNR of the entire sample. Use this value as a threshold.
3. Scan through array that holds SNR values and detect when the SNR rises above the threshold. Store array index of this point.
4. Continue scanning through the array and detect when the SNR falls below the threshold. Store array index of this point.
5. Using these array indexes, compute SNR *only* over this duration. Store SNR value in variable for later presentation.

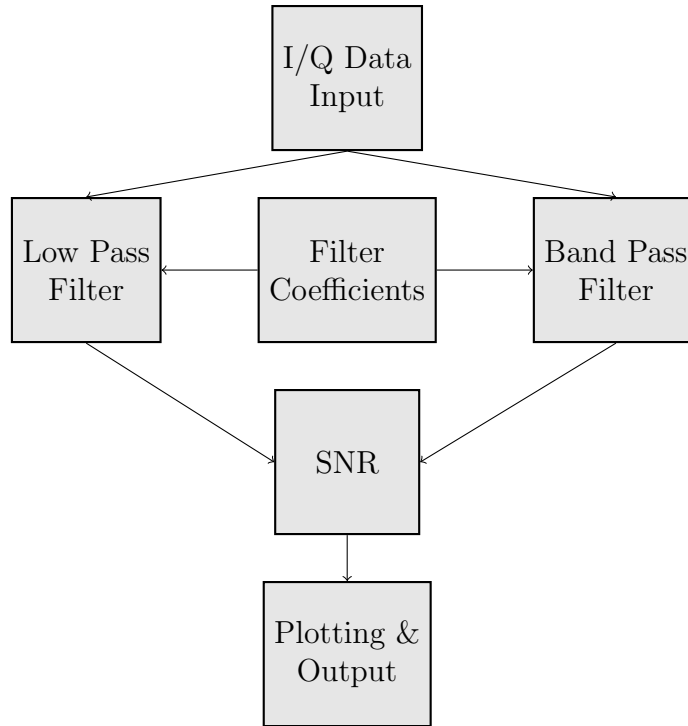


Figure 3: Program Flow for `snr_vs_time_batch_dat.m`

Using this method, the SNR is calculated only over the interval that the signal is present. In addition to this average, this script will also output a graph of the SNR over the duration of the entire recording. Although no definitive SNR data can be obtained from these graphs, they serve as a good qualitative aid for someone who wants to see how the SNR for each polarization changes over the duration of the signal and the sample. In many cases observed thus far, the SNR of different polarizations fluctuates wildly, and it is difficult to tell visually which polarization is the strongest. In these same cases, the average SNR value may not be meaningful, especially if all of the polarizations have similar SNR values.

The SNR is calculated in small time steps. This is adjustable in the MATLAB scripts. Currently, a time step of 0.1 second is used. Shorter steps could be used, at the expense of computation time and accuracy, but it is not clear what insight could be gained by using smaller time steps. Using smaller time steps will also not provide insight into fast fading, since fast fading is likely to occur on time scales comparable to the sample rate of the radio, or at least the symbol rate of the transmitted data. Thus it would be impossible to observe fast fading given the equipment and signals used.

3.5.2 Processing in the Presence of Interference

Naturally, some of the collected samples will contain interference in adjacent frequencies. This is to be expected for the samples of WWV since it uses frequencies close to international broadcast stations. It is beyond the scope of this experiment to write a comprehensive detection algorithm that can frequency shift the desired signals as necessary to avoid interference

in the designated noise sample or the negative frequencies which are also in the passband of the digital filter. Thus, samples which contain a good recording of either of these waveforms, but fail to be correctly processed in a batch processing script due to interference must be processed by manually altering the filters defined in the script. In order to keep the processing algorithm completely automatic, however, manual alteration of the filters will not be done for the actual tests.

3.5.3 Reconstruction of Circularly Polarized Waves

The current WBHF Testbed configuration allows for easy digital reconstruction of the circularly polarized components of the incoming wave. The system's dual receiver architecture allows the user to receive both left and right hand circular polarization without additional phasing hardware. So long as the antennas used are sufficiently wideband and configured perpendicular to one another, a software routine can perform this transformation.

If we consider the signals from each individual dipole to have a phase of 0 degrees, the task of constructing circular polarization seems somewhat trivial. One signal must simply be offset from the other by 90 degrees. For this to occur, the following matrix transformation is applied in software:

$$\begin{bmatrix} \text{RHCP} \\ \text{LHCP} \end{bmatrix} = \begin{bmatrix} j & 1 \\ 1 & j \end{bmatrix} \begin{bmatrix} I_1 + jQ_1 \\ I_2 + jQ_2 \end{bmatrix}$$

It is important to note that the data from each linearly polarized channel is complex valued. The transformation from two linearly polarized signal into one circularly polarized signal involves the sum of the linear channels, with one channel having its real and complex values interchanged: $a + jb \rightarrow -b + ja$. This operation is equivalent to rotating a vector 90 degrees in the complex plane. Thus this matrix operation become intuitive: if we have one vector oscillating with equal real and imaginary amplitudes in the complex plane, and we sum another similar vector that is rotated by 90 degrees, the resultant vector will trace a circle in the complex plane. This is circular polarization.

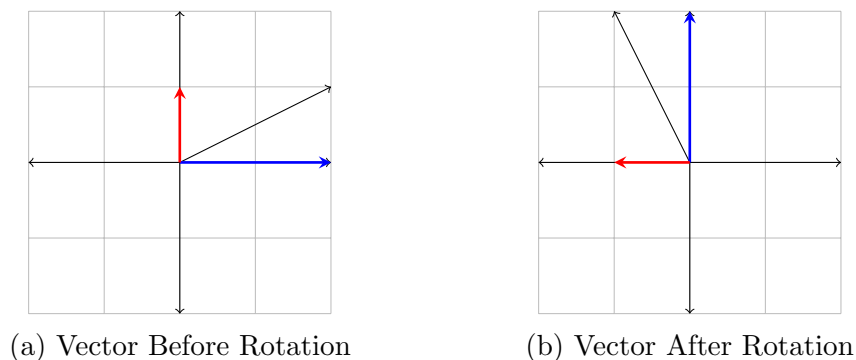


Figure 4: Example of Vector Rotation

4 Results

4.1 Preliminary Findings

4.1.1 WWV

The first of the reception tests were done with the time station WWV. These reception tests unfortunately did not provide any decisive data concerning SNR improvements. As a result of WWV's AM modulation scheme, the signal as a whole had a constantly changing envelope, which made the plots of SNR over time very difficult to interpret qualitatively or process automatically for an average. For other modulation formats, the constant envelope ensures that an average can be taken of the SNR during the transmission, which aids in automatic processing and data collection. The strength of the AM carrier could be used as the indicator of signal strength, since it does not vary in strength as quickly as the sidebands vary and is a better overall indicator. However, because of the mixing scheme of the WBHF, whereby everything is mixed down to baseband, the AM carrier would have been at DC. It was not clear how one would measure the strength of a DC amplitude using functions from the MATLAB Signal Processing Toolbox.

Nonetheless, by visual inspection it is easy to see that certain trends emerge over the duration of a sample. For most of the WWV samples, such as the ones shown in Figure 5, it can be seen that the SNR for the RHCP wave trends higher than the SNR for the other waves. It is unfortunate that this trend could not be extrapolated automatically, but human judgement will have to suffice in this case, since the WWV recordings serve only as a preliminary gauge.

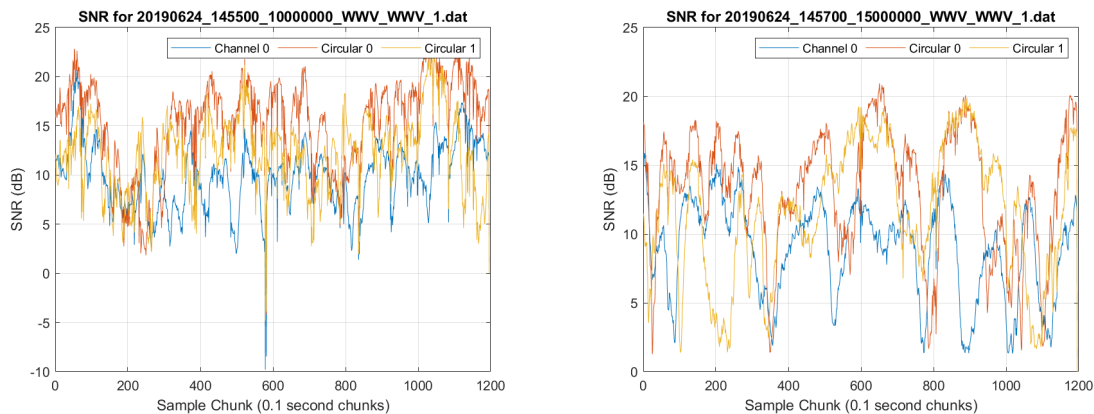


Figure 5: Two WWV Samples

4.2 Theoretical Improvements from Antenna Simulations

Simulated far field radiation patterns of the MITRE Crossed Dipole are another valuable indicator of the improvement that can be expected from using circularly polarized antennas. The MITRE Crossed Dipole was simulated using EZNEC and Altair Feko, which are two popular electromagnetics programs. EZNEC uses the classic Numerical Electromagnetics

Code (NEC) engine and the Method of Moments (MoM) technique to calculate the currents and fields for arbitrary wire geometries. It is a simpler program that is marketed primarily towards amateur radio operators and suited better for modelling wire antennas. Altair Feko is a much more advanced program which supports many more solving techniques, and thus it can model and analyze structures and materials with complex geometries and properties. The antenna was modelled in both programs so that the patterns could be compared for agreement.

As mentioned earlier, the MITRE Crossed Dipole is designed to enhance NVIS propagation. The Stockbridge-Bedford link that has been under test in this experiment is most likely supported only by ionospheric wave refraction at a high angle of incidence, or NVIS propagation. Thus it was decided that it would be more insightful to generate elevation patterns rather than azimuth patterns. Those will be included in the following subsections.

All elevation patterns are generated at both 5 and 7 MHz. All test transmissions took place between these frequencies and thus it was decided that generating patterns at these frequencies would give adequate insight into the radiation patterns of both antennas.

4.2.1 EZNEC Model

The EZNEC generated elevation patterns clearly show that this is antenna optimized for NVIS propagation. The majority of the field is concentrated vertically, with diminishing radiation at lower elevation angles. More importantly, the patterns show that this antenna has good isolation between the right hand and left hand circular polarizations. At 5 MHz, the isolation is on the order of 30 dB at zenith and reaches a minimum of 16 dB at low takeoff angles. Conveniently, the angle of minimum isolation occurs outside of the antenna's -3 dB bandwidth, which is denoted by the purple lines. At 7 MHz, the isolation at zenith is slightly reduced to about 22 dB, and at low angles it falls to minimum of about 12 dB.

The excitation to this antenna was phased in such a way that right hand circular polarization would be produced. The phases can be switched if left hand circular polarization is desired. The results will be identical, but swapped.

In addition to good polarization isolation, the total field plots (shown on the right) also indicate that the total emitted wave is polarized dominantly in one circular polarization. This is evident by the identical shape and amplitude of the right hand circular and total field patterns.

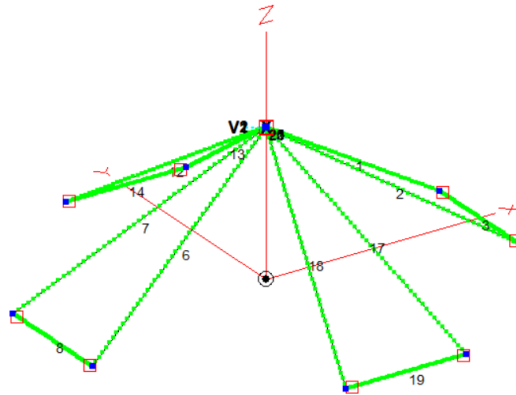


Figure 6: EZNEC Model of the MITRE Crossed Dipole

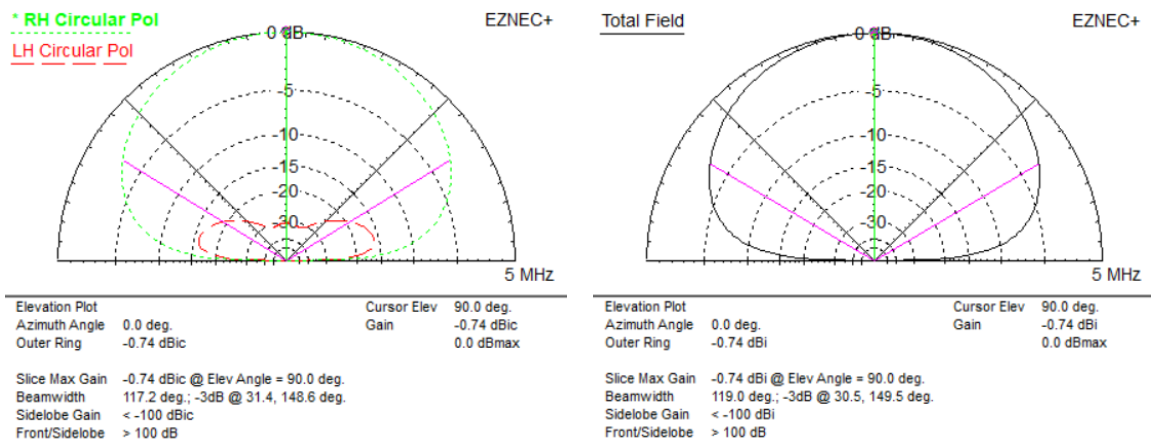


Figure 7: MITRE Crossed Dipole Elevation Far Field, 5 MHz

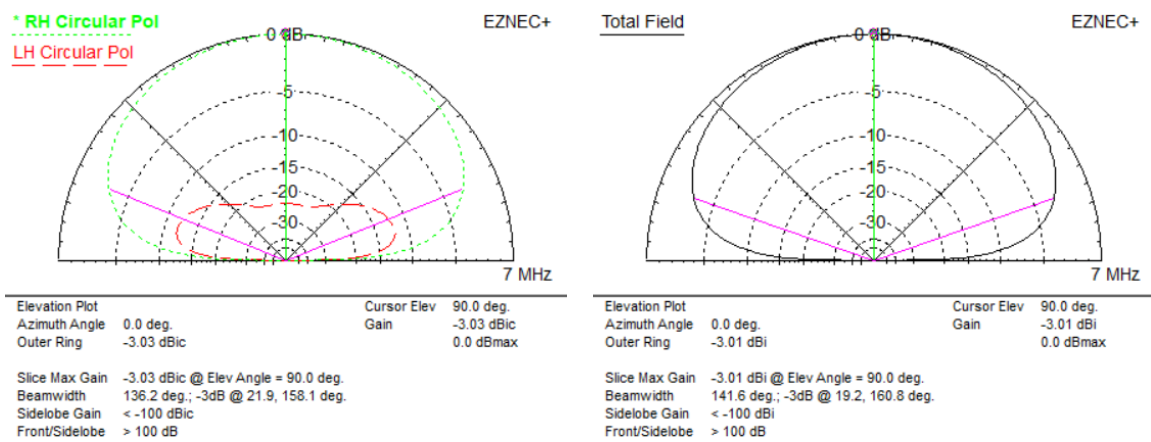


Figure 8: MITRE Crossed Dipole Elevation Far Field, 7 MHz

4.2.2 Altair Feko Model

The Feko model for the crossed dipole agrees with the results from the EZNEC simulations.

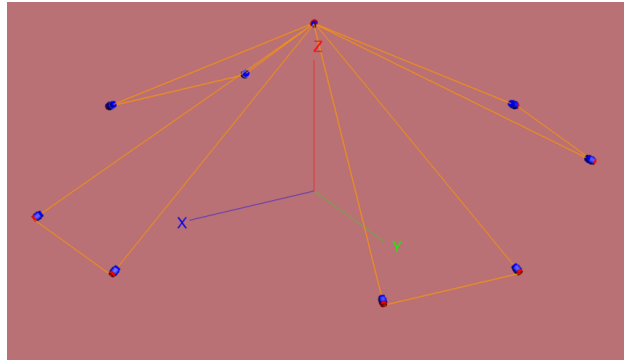


Figure 9: Feko Model of the MITRE Crossed Dipole

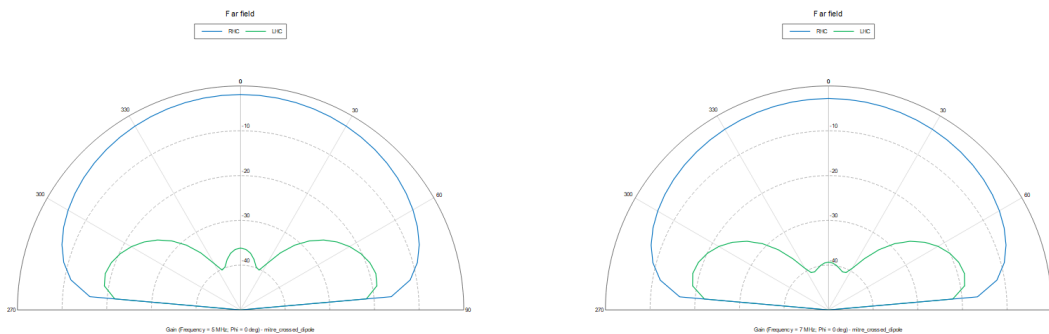


Figure 10: MITRE Crossed Dipole Elevation Far Field, 5 & 7 MHz

The Feko-generated patterns do not look exactly the same as the EZNEC patterns because the graph scales are slightly different. The radial scale in the EZNEC output is not uniform, and unfortunately this could not be changed because there was no option to do so within EZNEC. Inspection of the plots shows that at zenith there is a polarization isolation of 35 and 39 dB at 5 and 7 MHz respectively. This is several dB greater than the EZNEC results. The isolation at its minimum value was approximately 18 dB in both cases, which is also greater by several dB than what EZNEC predicted.

The difference in the results can possibly be attributed to the solving techniques used by each program. EZNEC uses the Method of Moments exclusively, while Feko can utilize 9 different solvers [12]. Feko also can choose to take a hybrid approach to solving a structure, whereby it uses a combination of different methods to produce a more accurate results. It is believed that this is the cause of the discrepancy between the results. It is also for this reason that the Feko results are believed to be more accurate than the EZNEC results.

4.3 Test Results

4.3.1 Reception with Software Reconstruction of Circular Polarization

The receiving and transmitting system was set up as described in Section 3.3. The samples in each sample set were taken successively on a single day. It was found that circular polarization yielded signal to noise improvements of approximately 1 to 4 dB over the strongest linear polarization. For many of the tests, it can be seen that the dominant circular polarization is in fact right hand. In only one test, however, was left hand polarization dominant.

There were several tests where linear polarization was actually stronger than either circular polarization. Circular polarization is not a universal solution for improving signal to noise ratio. It is entirely probable that the electromagnetic wave will not be split appreciably as it reflects off of the ionosphere and thus rejecting a circular component will not have any distinct advantages over simply receiving with a linear antenna. In fact, it might cause a significant disadvantage because a circularly polarized antenna will receive a linearly polarized wave with a -3 dB loss in the signal strength. [13] In the case of this experiment, that loss is not incurred because the two halves of the MITRE crossed dipole technically act as two independent linear antennas. For that reason, the calculated SNRs for the linear samples are still accurate.

It should be noted that several tests have SNRs for each polarization close to or below 0 dB. These are not the actual average signal strengths, calculated according to the method described in Section 3.5.1. These SNR calculations are inaccurate due to the admittedly simplistic detection algorithm. Several of these samples were inspected manually and were found to have a widely fluctuating SNR which went below the detection threshold and triggered the “end of the sample” condition. Thus, the SNR was likely calculated over a very short duration which was not representative of the true average SNR. Therefore, these samples must be omitted so that each sample may be processed in a consistent manner.

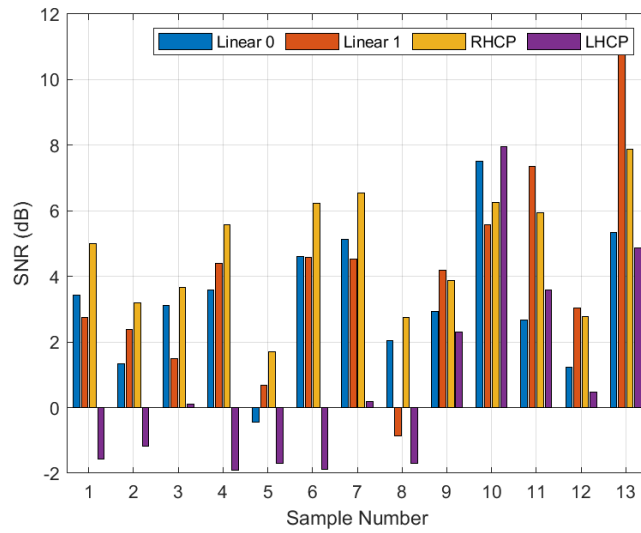


Figure 11: Data From Test on September 12, 2019

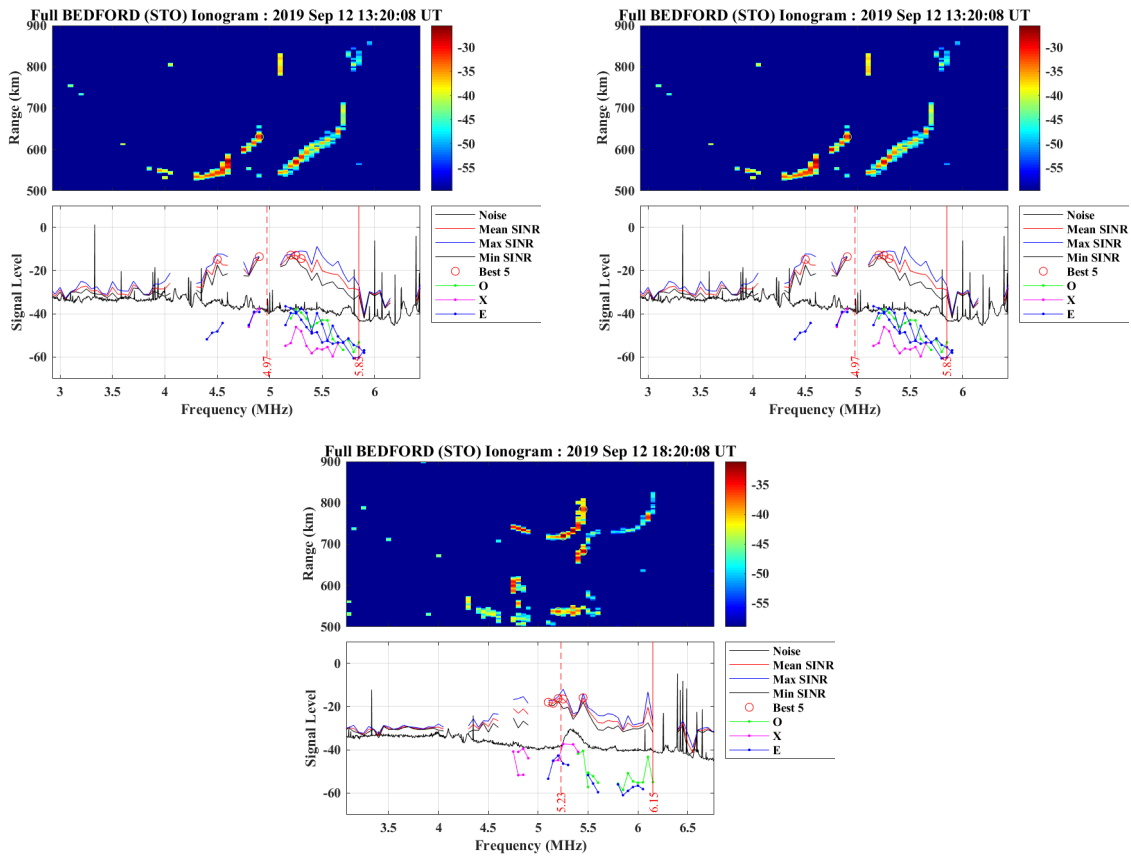


Figure 12: Ionograms During September 12 Tests

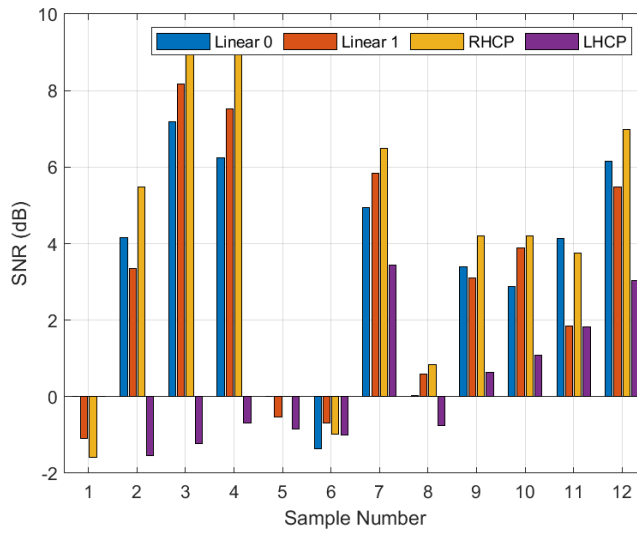


Figure 13: Data From Test on September 20, 2019

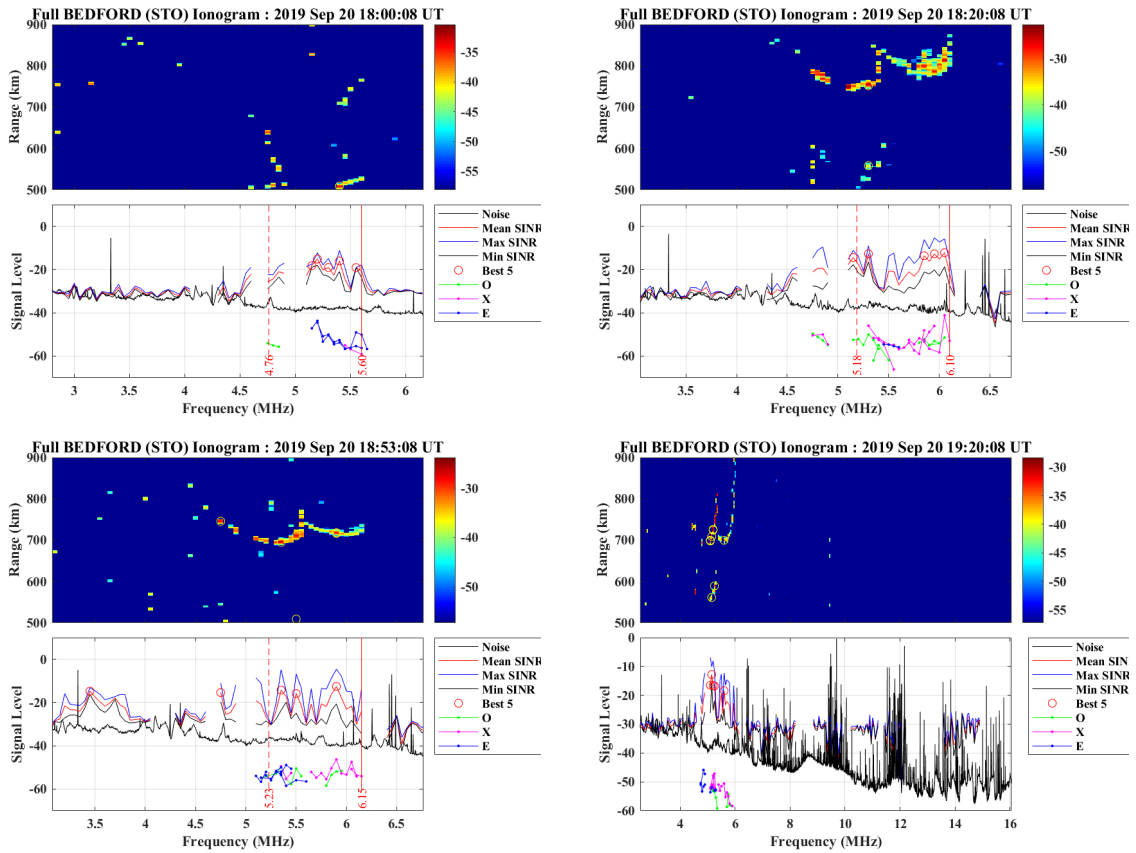


Figure 14: Ionograms During September 20 Tests

4.3.2 Reception with 0-90 Hybrid

A second field test was also performed using a 0-90 hybrid to simulate a real usage scenario. The receiver was configured as described in Section 3.4.3. The results of this test are expected to correspond with the results from the test using digital reconstruction of the wave. All of the results in the following table are in units of dB, if not otherwise noted.

Test #	MHz	X #1	Linear	X #2	O	X #3	X _{avg}	X _{avg} - Linear	Δ O
1	4.8	7	5	4.5	-2	5	5.5	0.5	7.5
2	5.2	7	7	6	4.5	5.5	6.16	-0.84	1.66
3	5.35	6.5	4	4	4	6	5.5	1.5	1.5
4	5.5	7	7	6	7	7	6.66	-0.34	-0.34

It can be seen from this table that for most of the tests favoring X mode, the SNR is greater than the SNR from the tests that favor O mode or use linear polarization. For two of the four tests, the average X mode SNR was greater than the SNR using linear polarization. Due to time constraints, it was not possible to collect more samples than this. However, if more samples were taken, we would expect to see the trend agree with that of the tests using the WBHF SDR, where the average trended towards a higher SNR when favoring X mode over linear polarization.

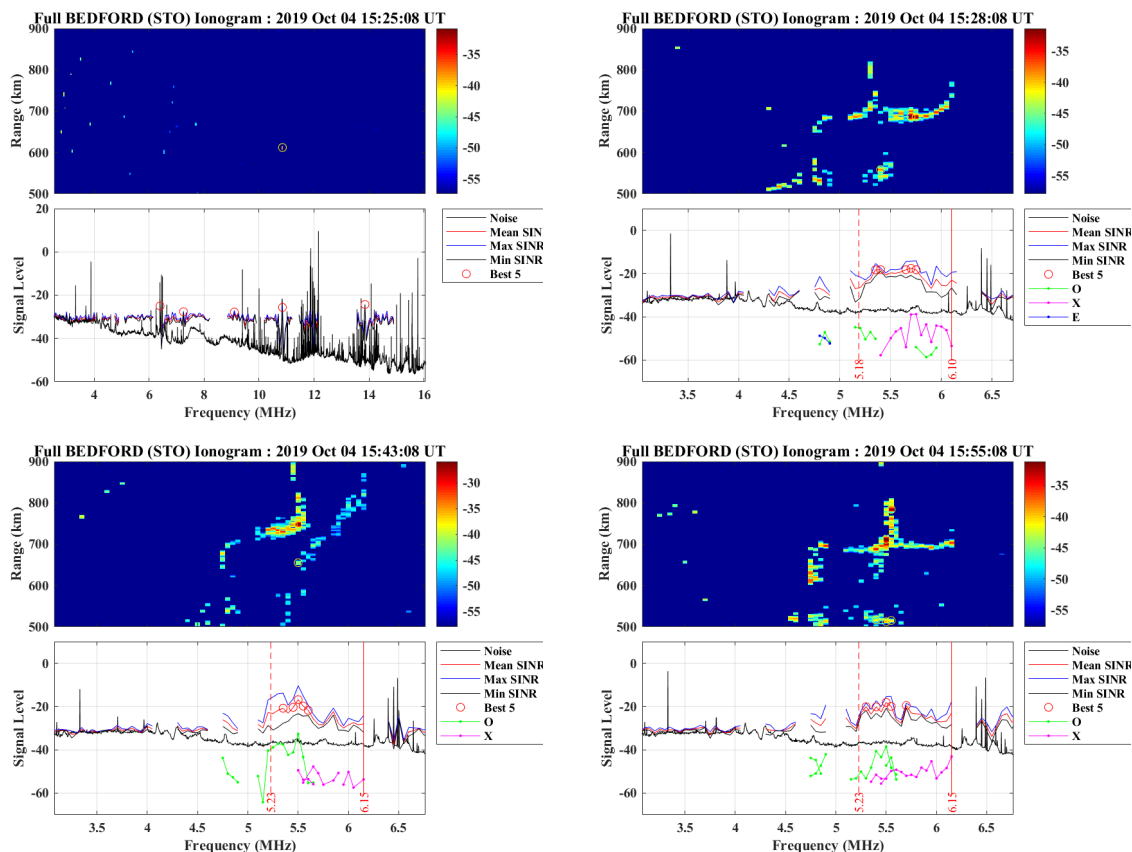


Figure 15: Ionograms During Tests with 0-90 Hybrid

5 Conclusions and Recommendations

From the data, it is clear that in many of the test transmissions circular polarization yielded a maximum SNR improvement of approximately 3 dB over the strongest channel using linear polarization. A 3 dB improvement is a non-negligible increase in signal strength, which roughly translates to a doubling of the effective range of the HF link. Although the SNR degradation due to polarization fading could not be measured directly, the tests show that the SNR performance of this link did improve when circular polarization was in use. It is unlikely that the differences in SNR between linear and circular polarization can be attributed to something other than polarization fading, given that the only change between them was the polarization of the antenna.

Although right hand circular polarization was dominant in these tests, the usage of left hand circular polarization should also be considered. Given simple phasing methods, it is not difficult to construct a ground based antenna system that would allow for switching between RHCP and LHCP. If the radios in a hypothetical HF link are operated manually, the operators could choose a polarization based on a test transmission scheme similar to the one used in this experiment.

It is therefore recommended that whenever the operating situation allows, a circularly polarized antenna should be used. The current state of the portable HF antenna market is not known; nor is the author aware of any ground based HF antennas that are designed to emit circular polarization (outside of the MITRE crossed dipole used in this experiment). However if there is such a wire antenna that is portable, wideband, and suitable for HF work, it could be readily adapted to emit circular polarization if two such antennas were used. The configuration would follow that of the MITRE crossed dipole: having the two antennas oriented perpendicular to one another and phased to emit the desired circular polarization.

Such an idea was tested using the White Wolf Systems “Whiskey” antenna. It is a broadband HF wire antenna which is optimized for NVIS propagation. White Wolf Systems designed this antenna for tactical field use and for this reason it is easily set up and taken down. The original design makes no mention of using two antennas to generate circular polarization. To explore this idea, the antenna geometry was measured using an antenna set up in the field. Not all length information was given in the manual or design document. The geometry was entered into both EZNEC and Altair Feko and characterized for input impedance and radiation pattern. This data can be found in Appendix A. The antenna has similar radiation patterns, comparable mode isolation, and a somewhat larger impedance bandwidth when compared to the MITRE Crossed Dipole. Another study could be done to assess the performance of using current off-the-shelf HF wire antennas for this purpose.

Bibliography

- [1] RadioReference.com. (). USAF High Frequency Global Communications System, [Online]. Available: https://wiki.radioreference.com/index.php/USAF_High_Frequency_Global_Communications_System. (accessed: 08.26.2019).
- [2] “IEEE Standard Definitions of Terms for Radio Waves Propagation”, *IEEE Std 211-2018 (Revision of IEEE Std 211-1997)*, pp. 1–57, Feb. 2019. DOI: [10.1109/IEEESTD.2019.8657413](https://doi.org/10.1109/IEEESTD.2019.8657413).
- [3] D. R. Williams. (2019). Earth Fact Sheet, [Online]. Available: <https://nssdc.gsfc.nasa.gov/planetary/factsheet/earthfact.html>.
- [4] K. Davies, *Ionospheric radio*, eng, ser. IEE electromagnetic waves series ; v. 31.. London: Peregrinus on behalf of the Institution of Electrical Engineers, 1989, ISBN: 086341186X.
- [5] Phirosiberia. (2009). Ionosphere layers en, [Online]. Available: https://commons.wikimedia.org/wiki/File:Ionosphere_Layers-en.svg.
- [6] S. W. P. Center. (). Solar Flares (Radio Blackouts), [Online]. Available: <https://www.swpc.noaa.gov/phenomena/solar-flares-radio-blackouts>.
- [7] Dave3457. (2010). Circular.polarization.circularly.polarized.light without.components right.handed, [Online]. Available: <https://commons.wikimedia.org/wiki/File:Circular.Polarization.Circularly.Polarized.Light.Without.Components.Right.Handed.svg>.
- [8] —, (2010). Circular.polarization.circularly.polarized.light without.components left.handed, [Online]. Available: <https://commons.wikimedia.org/wiki/File:Circular.Polarization.Circularly.Polarized.Light.Without.Components.Left.Handed.svg>.
- [9] B. Witvliet, E. van Maanen, G. Petersen, A. Westenberg, M. Bentum, C. Slump, and R. Schiphorst, “The importance of circular polarization for diversity reception and mimo in nvis propagation”, English, in *2014 8th European Conference on Antennas and Propagation (EuCAP)*, United States: IEEE, Apr. 2014, pp. 2797–2801. DOI: [10.1109/EuCAP.2014.6902407](https://doi.org/10.1109/EuCAP.2014.6902407).
- [10] MathWorks. (2019). FFT Based FIR filtering using overlap-add method - MATLAB fftfilt, [Online]. Available: <https://www.mathworks.com/help/signal/ref/fftfilt.html>.
- [11] Mathworks. (2019). Signal to noise ratio - MATLAB snr, [Online]. Available: <https://www.mathworks.com/help/signal/ref/snr.html>.
- [12] JIF. (2017). How to decide which numerical technique to use in FEKO? #2, [Online]. Available: <https://forum.altair.com/topic/20531-how-to-decide-which-numerical-technique-to-use-in-feko/>.
- [13] (). Electronic Warfare and Radar Systems Engineering Handbook - Polarization, [Online]. Available: <http://www.rfcafe.com/references/electrical/ew-radar-handbook/polarization.htm>.

Appendices

A White Wolf Systems “Whiskey” Antenna

This section will provide graphs of the elevation patterns and Standing Wave Ratio for the “Whiskey” Antenna manufactured by White Wolf Systems. This antenna is a good candidate for use in a circularly polarized configuration. This model takes two separate antennas and orients them perpendicular to one another. Each antenna is phased such that RHCP is generated.

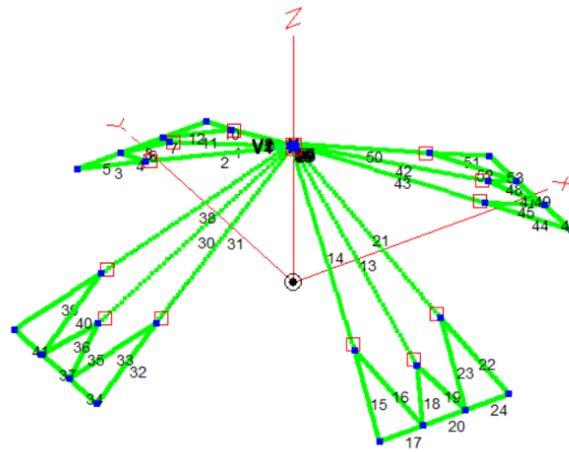


Figure 16: EZNEC Model of the Whiskey Antenna

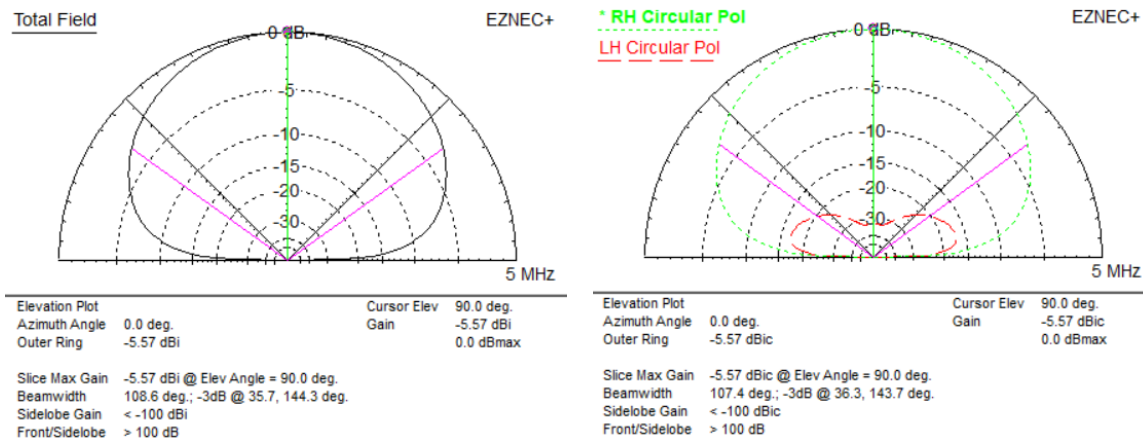


Figure 17: Whiskey Elevation Far Field, 5 MHz

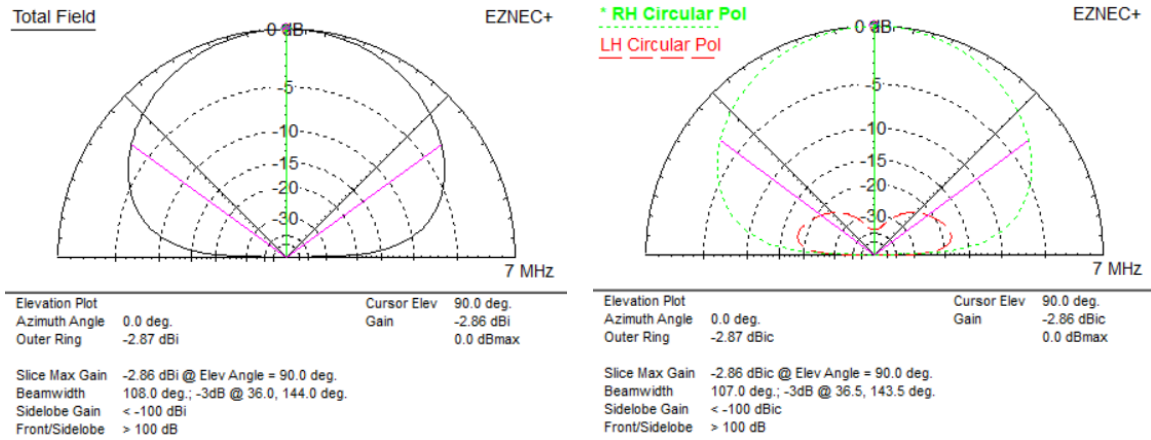


Figure 18: Whiskey Elevation Far Field, 7 MHz

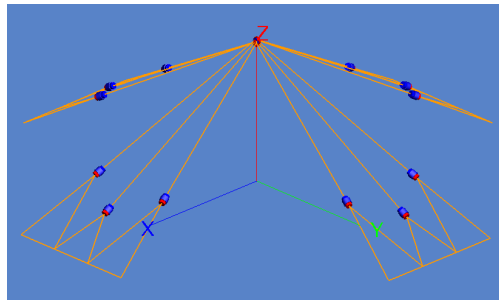


Figure 19: Feko Model of the Whiskey Antenna

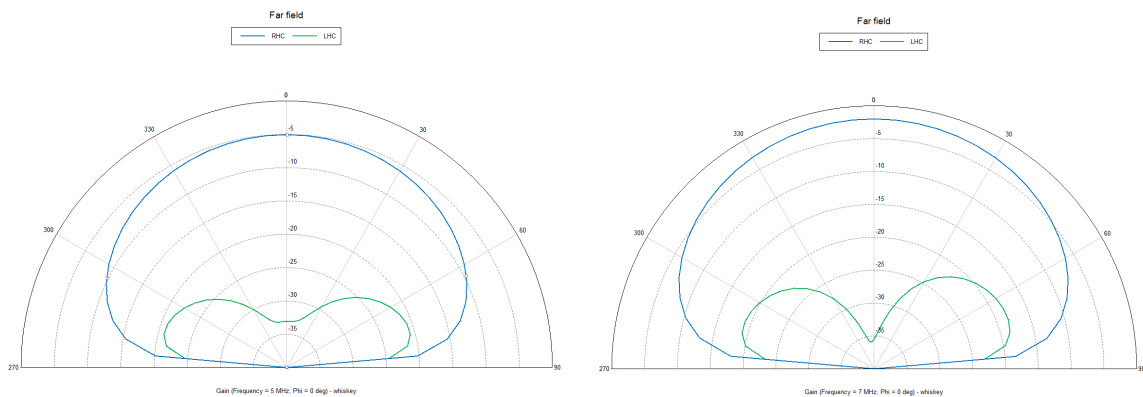


Figure 20: Whiskey Elevation Far Field, 5 & 7 MHz

B MATLAB Scripts

```

1 % Modified SNR vs Time for use with DAT files
2 % The process of reading in the DAT files is different because they
3 % have headers and the data is structured differently, and there is no
4 % convenient function like 'wavread' to do the work for you.
5
6 disp('Reading all DAT files from current directory');

```

```

7 files = dir('*.dat');
8
9 % Make sure you set a directory in which all the plot images can go.
10 if 7 == exist('plots', 'dir')
11     disp('Plot folder found');
12     plotdir = './plots/';
13 else
14     plotdir = input('Plot folder not found. Please specify directory for
plots:', 's');
15 end
16
17 % Define filters
18 lp = 3.2e3;
19 Fs = 200e3;
20 signal_filt = designfilt('lowpassfir', 'PassbandFrequency', lp/Fs, '
StopbandFrequency', (lp+0.2e3)/Fs, 'PassbandRipple', 1, '
StopbandAttenuation', 60);
21 noise_filt = designfilt('bandpassfir', 'FilterOrder', 200, '
CutoffFrequency1', 8e3, 'CutoffFrequency2', 11.2e3, 'SampleRate', Fs);
22
23 b = 1; % counter for final output data
24
25 for k = 1:2:length(files)
26     % BEGIN CHANNEL 0 PROCESSING
27     % Read file, import data
28     arg = files(k).name;
29     fileID = fopen(arg);
30     size = fread(fileID, 1, 'uint32');
31     freq = fread(fileID, 1, 'double');
32     Fs = fread(fileID, 1, 'double');
33     start_time = fread(fileID, 1, 'uint64');
34     temp = fread(fileID, 'int16=>double');
35     iqdata0 = zeros(1, length(temp)/2);
36     y = 1;
37     for x = 1:2:length(temp)-1
38         iqdata0(y) = complex(temp(x), temp(x+1));
39         y = y + 1;
40     end
41     fclose(fileID);
42
43     % Filter signal, noise
44     ch0 = fftfilt(signal_filt, iqdata0);
45     noise0 = fftfilt(noise_filt, iqdata0);
46
47     % interval = input('Type the interval in seconds over which the SNR
will be taken\n');
48     interval = 0.1;
49     % we need to know the amount of samples to run through on each loop
50     samples_per_loop = floor(Fs*interval);
51     x = 1;
52     snrdata0 = zeros(1, ceil(length(ch0)/samples_per_loop));
53     % step through array using number of steps calculated
54     for y = 1:samples_per_loop:length(ch0)-samples_per_loop
55         if y == length(ch0)

```

```

56         break;
57     end
58     % calculate snr
59     % while doing so, situate all snr values into an array
60     snrdata0(x) = snr(ch0(y:y+samples_per_loop), noise0(y:y+
samples_per_loop));
61     % make separate variable for data index
62     x = x + 1;
63 end
64 % clear everything except the combined IQ data and the SNR data
65 clear rawdata0 info ch0 noise0 temp fileID size freq;
66 % END CHANNEL 0 PROCESSING
-----

67
68 % BEGIN CHANNEL 1 PROCESSING
-----

69 arg = files(k+1).name;
70 fileID = fopen(arg);
71 size = fread(fileID, 1, 'uint32');
72 freq = fread(fileID, 1, 'double');
73 Fs = fread(fileID, 1, 'double');
74 start_time = fread(fileID, 1, 'uint64');
75 temp = fread(fileID, 'int16=>double');
76 iqdata1 = zeros(1, length(temp)/2);
77 y = 1;
78 for x = 1:2:length(temp)-1
79     iqdata1(y) = complex(temp(x), temp(x+1));
80     y = y + 1;
81 end
82 fclose(fileID);
83
84 % filter signal, noise
85 ch1 = fftfilt(signal_filt, iqdata1);
86 noise1 = fftfilt(noise_filt, iqdata1);
87
88 % interval = input('Type the interval in seconds over which the SNR
will be taken\n');
89 % due to decimal errors, let's keep it at 1 second for now
90 interval = 0.1;
91 % we need to know the amount of samples to run through on each loop
92 samples_per_loop = floor(Fs*interval);
93 x = 1;
94 snrdata1 = zeros(1, ceil(length(ch1)/samples_per_loop));
95 % step through array using number of steps calculated
96 for y = 1:samples_per_loop:length(ch1)-samples_per_loop
97     if y == length(ch1)
98         break;
99     end
100     % calculate snr
101     % while doing so, situate all snr values into an array
102     snrdata1(x) = snr(ch1(y:y+samples_per_loop), noise1(y:y+
samples_per_loop));
103     % make separate variable for data index
104     x = x + 1;

```

```

105     end
106     % clear everything except the combined IQ data, SNR data and file
argument
107     clear rawdata1 ch1 info noise1 temp fileID size freq;
108     % END CHANNEL 1 PROCESSING
-----

109
110     % BEGIN CIRCULAR PROCESSING
-----

111     ch0_circular = iqdata0*1j + iqdata1; % right hand
112     ch1_circular = iqdata0 + iqdata1*1j; % left hand
113     ch0_filtered = fftfilt(signal_filt, ch0_circular);
114     ch1_filtered = fftfilt(signal_filt, ch1_circular);
115     ch0_noise = fftfilt(noise_filt, ch0_circular);
116     ch1_noise = fftfilt(noise_filt, ch1_circular);
117     snrdata_circular0 = zeros(1, ceil(length(ch0_filtered)/
samples_per_loop));
118     snrdata_circular1 = zeros(1, ceil(length(ch1_filtered)/
samples_per_loop));

119
120     x = 1;
121     % step through array using number of steps calculated
122     for y = 1:samples_per_loop:length(ch0_filtered)-samples_per_loop
123         if y == length(ch0_filtered)
124             break;
125         end
126         % calculate snr
127         % while doing so, situate all snr values into an array
128         snrdata_circular0(x) = snr(ch0_filtered(y:y+samples_per_loop),
ch0_noise(y:y+samples_per_loop));
129         % make separate variable for data index
130         x = x + 1;
131     end
132
133     x = 1;
134     % step through array using number of steps calculated
135     for y = 1:samples_per_loop:length(ch1_filtered)-samples_per_loop
136         if y == length(ch1_filtered)
137             break;
138         end
139         % calculate snr
140         % while doing so, situate all snr values into an array
141         snrdata_circular1(x) = snr(ch1_filtered(y:y+samples_per_loop),
ch1_noise(y:y+samples_per_loop));
142         % make separate variable for data index
143         x = x + 1;
144     end
145     % clear IQ data and such, keep SNR data
146     clear ch0_circular ch1_circular ch0_filtered ch1_filtered ch0_noise
ch1_noise iqdata0 iqdata1
147     % END CIRCULAR PROCESSING
-----

148
149     % Average SNR calculations

```

```

150     snrdata.channel0(b) = avg_snr(snrdata0);
151     snrdata.channel1(b) = avg_snr(snrdata1);
152     snrdata.circ0(b) = avg_snr(snrdata_circular0);
153     snrdata.circ1(b) = avg_snr(snrdata_circular1);
154     b = b + 1;
155
156     % Save plot of data without opening the figure in a window
157     f1 = figure('Visible', 'off');
158     % plot(1:x, snrdata0(1,:), 1:x, snrdata_circular0(1,:), 1:x,
snrdata_circular0(1,:), 1:x, snrdata_circular1(1,:));
159     plot(1:x, snrdata0(1,:), 1:x, snrdata1(1,:), 1:x, snrdata_circular0
(1,:), 1:x, snrdata_circular1(1,:));
160     grid on;
161     xlabel(['Sample Chunk' ' (' num2str(interval) ' ' 'second chunks)']);
162     ylabel('SNR (dB)');
163     % a little string processing for the title
164     dat_name = string(strsplit(arg, '.dat'));
165     title(strcat('SNR for', {' '}, dat_name(1)), 'Interpreter', 'none');
166     % legend('Channel 0', 'Channel 1', 'Circular');
167     legend('Linear 0', 'Linear 1', 'RHCP', 'LHCP', 'NumColumns', 4, '
Location', 'southeast');
168     saveas(f1, strcat(plotdir, dat_name(1), '.png'));
169
170     disp(strcat('File ', {' '}, dat_name(1), ' has been processed.));
171     % clean everything up
172     clear ch0_circular ch1_circular ch0_filtered ch1_filtered ch0_noise
ch1_noise snrdata_circular0 snrdata_circular1 dat_name snrdata0
snrdata1
173 end
174
175 % Finally, take the snrdata and output a barchart
176 y = [snrdata.channel0' snrdata.channel1' snrdata.circ0' snrdata.circ1'];
177 bar(y);
178 xlabel('Sample Number'); ylabel('SNR (dB)');
179 legend('Linear 0', 'Linear 1', 'RHCP', 'LHCP', 'NumColumns', 4);
180 grid on;
181 saveas(gcf, strcat(plotdir, 'barchart.png'));

```

snr_vs_time_batch_dat.m

```

1
2 % Average SNR calculations
3 % This function should take in the SNR array that is output to the graphs
4 function snr = avg_snr(input_array)
5     threshold = mean(input_array);
6
7     x = 1;
8     % detect when the signal begins
9     while x < length(input_array)
10         if input_array(x) > threshold
11             start = x;
12             break;
13         end
14         x = x + 1;

```

```

15     end
16     if ~exist('start', 'var')
17         disp('Start of signal not found');
18         snr = 0; % return 0 snr if it cannot be calculated
19         return;
20     end
21
22     % detect when the signal ends
23     for x = start:length(input_array)
24         if input_array(x) < threshold
25             finish = x;
26             break;
27         end
28     end
29     if ~exist('finish', 'var')
30         disp('End of signal not found');
31         snr = 0; % return 0 snr if it cannot be calculated
32         return;
33     end
34     % take average of SNR
35     snr = mean(input_array(start:finish));
36 end

```

avg_snr.m